Performance Evaluation of Multipath Mitigation Techniques for Critical Urban Applications Based on a Land Mobile Satellite Channel Model

Philippe Brocard, Daniel Salós, Olivier Julien, Mikaël Mabilleau

▶ **To cite this version:**

HAL Id: hal-00989822

https://hal-enac.archives-ouvertes.fr/hal-00989822

Submitted on 29 Jun 2016

Performance Evaluation of Multipath Mitigation Techniques for Critical Urban Applications Based on a Land Mobile Satellite Channel Model

Philippe Brocard, Daniel Salos, Olivier Julien
Ecole Nationale de l'Aviation Civile
Toulouse, France
brocard@recherche.enac.fr

Mikael Mabilleau
Egis Avia
France

Abstract—**The use of GNSS for critical terrestrial applications requires adapted integrity monitoring algorithms for either safety or liability issues. Prior to the design of integrity monitoring algorithms, it is necessary to characterize the nominal error model of every error source affecting the pseudorange measurements. This paper focuses on describing a way to calculate the contribution of the multipath to the nominal error model by a set of simulations based on an urban channel model and a realistic GNSS tracking loop simulator. To improve the accuracy of the positioning, multipath mitigation techniques are usually implemented in the receivers. This paper assesses the performances of the Narrow Correlator, the Double-Delta and the A Posteriori Multipath Estimation techniques in an urban environment and provides their multipath residual nominal error model as a function of the satellite elevation angle. A relationship between quality monitoring indicators and the multipath estimation technique (APME) is also discussed. The results of this paper are obtained by simulating an actual urban railway environment and therefore can be taken as inputs for the design of GNSS integrity monitoring algorithms for rail users. The same approach can be used for the determination of the nominal error model for other terrestrial application subject to simulating an adapted channel.**

Keywords—multipath mitigation; urban environment; error model; rail users

I. INTRODUCTION

Due to the modernization of current GNSS, the development of new GNSS like Galileo and Beidou, and the improvement of Satellite Based Augmentations Systems (SBAS), GNSS is a promising alternative for terrestrial rail and road position monitoring systems that require costly ground infrastructures.

In the rail domain, the European Train Control System (ETCS) [1] is the automatic signaling, control and train protection system that is currently being deployed for an improved interoperability in Europe. In ETCS level 2 and 3 the vehicles have to self-monitor their position and speed, based on a combination of radiobeacons (Eurobalises) installed along the railway that provide reference positions, and odometry. Several European projects have investigated the possible introduction of GNSS in ETCS to reduce the number of radiobeacons that currently has to be at least one per 2.5 km

[1]. Among these projects, it can be mentioned INTEGRAIL (ESA, 2001), GRAIL (6th FP, GSA, 2005), GRAIL-2 (7th FP, GSA, 2010), 3INSAT (ESA, 2012) and SATLOC (7th FP, GSA, 2012). The memorandum of understanding between the European Commission and the European Rail sector Association (ERA) of 2012 states that "GNSS can play a major role in the rail sector for fleet management and rail safety". To speed up the standardization process for the use of GNSS in ETCS, the Union Industry of Signalling (UNISIG) created a working group called Satellite Positioning Working Group in cooperation with the European GNSS Agency (GSA). The main challenge for the introduction of the GNSS in train control is the very low Tolerable Hazard Risk (THR), which, for the whole signaling system, shall not be over 2.10^{-9}/h to fulfill the SIL4 requirement [1]. Therefore, the tolerable uncertainty on the GNSS position solution shall be even lower, as referred in [2] which mentions a THR between 1.10^{-10}/h and 1.10^{-11}/h, [3] that mentions a THR between 1.10^{-11} and 1.10^{-12}/h, [4] that sets the Integrity risk at 4.10^{-12}/h, and [5] THR = 1.10^{-11}/h. These operational requirements are far more stringent than the performances of the existing standalone GNSS, therefore the use of an adapted integrity monitoring concept is required.

In the road domain, GNSS is one of the recommended technologies in the EU directive for Electronic Toll Collection (ETC) [6] and GNSS based ETC systems already exists for heavy good transportation in Germany (Toll Collect) and Slovakia (MYTO). The norm CEN ISO TS 17444-1 provides different metrics that allow to define and assess the performance of ETC systems in terms of overcharging and undercharging. GNSS integrity monitoring systems can be used in ETC in order to enhance the liability of the charging system.

GNSS based ETC and Train Control are two examples of terrestrial applications that require their own integrity monitoring concepts to augment the GNSS and to fulfill their operational requirements. The design of such algorithm shall be adapted to the system and take into account the available sensors, augmentations systems, and the integrity requirements to real-time monitor the protection levels. Prior to the design of any integrity monitoring algorithm, it is necessary to

characterize the nominal error model of every error sources affecting the pseudorange measurements. For both applications, the vehicles are likely to operate in urban area where the multipath is a significant contributor to the error measurement.

This paper aims at characterizing the nominal code pseudorange multipath error standard deviation in urban environments for rail users with dual constellation GPS/Galileo single-frequency L1/E1 receivers. To do so, the characterization is based on the use of the wideband Land Mobile Satellite (LMS) channel model developed by the German Aerospace Center (DLR). This model is the reference wideband model for the ITU (International Telecommunication Union). Based on an urban railway channel scenario, the code measurements' statistics and residual errors are investigated using standard tracking loops as well as several multipath mitigation techniques. The channel simulated in this paper represents a typical urban railway environment, therefore the provided results apply to rail users. The same approach could be used to determine the nominal pseudorange error model for ETC by modifying the scenario.

II. DESCRIPTION OF SIMULATION TOOLS

The approach consists in connecting a simulator of urban channel that generates time series of signal with a realistic GNSS receiver simulator.

A. LMS channel model

The Land Mobile Channel (LMS) model [7] which can be downloaded for free, is a generative wideband urban channel model based on a measurement campaign conducted in Munich in 2002. Compared to a narrowband model such as the one developed in [8], a wide band model assumes that the coherence time of the channel is negligible compared to the chip duration of the Pseudo Random (PRN) code. A wideband model is preferred in this paper in order to realistically simulate the impact of multipaths on the receivers tracking loops and therefore on the pseudorange measurement. The model simulates the received signal for a fixed satellite whose relative position to the user is characterized by its azimuth and its elevation. The used LMS model simulates the channel for a vehicle moving along a street with predefined parameters. The model generates differently the direct satellite to receiver Line-of-Sight (LOS) and the multipaths. The properties of the LOS are deterministically generated by simulating realistic physical phenomena. The diffraction of the LOS over the edges of the buildings, the shadowing induced by trees and the diffraction over lamp posts are considered. The echoes are statistically generated based on several distributions deduced from the measurement campaign. The number of reflections, the geometric distribution of the reflectors (from which the phase and delay are deduced), the power distribution of the echoes, their lifespan (space life duration) and the distribution of the time variation of their amplitude (fading) are used to generate the echoes.

At every sample (k), each received LOS and echo is characterized by its amplitude $\alpha_n(k)$, code delay $\tau_n(k)$ and carrier phase $\varphi_n(k)$. The model of the received signal is:

$$s(k) = \sum_{n=1}^{N} \alpha_n(k)d(kT_s - \tau_n(k))c(kT_s - \tau_n(k))\cos(\varphi_n(k)) \quad (1)$$

Where c is the spreading code, d is the GNSS data and T_s is the sampling period.

A slight modification was added to the original LMS model in order to consider the dynamic of the mobile in the generation of the code delay. In the original model, the delay of the LOS remains null even when considering a fixed satellite and a moving vehicle. To model the impact of the dynamic on the delay, a delay variation was added to both the LOS and echo to LOS relative delay. This phenomenon is referred to as code Doppler which has the same origin as the carrier Doppler. The additional delay variation for two consecutive samples k and $k+1$ is expressed by:

$$\tau(k+1) - \tau(k) = \frac{v_r}{c}.T_s \quad (2)$$

Where v_r is the derivative of the distance between the receiver and the satellite.

B. GNSS tracking simulator

A realistic GNSS receiver simulator, developed by ENAC and referred to as GeneIQ, uses the outputs of the LMS channel model, consisting of the times series containing the amplitude, code delay, carrier phase and Doppler of each LOS and reflections. This simulator is based on the modeling of the receiver correlator outputs which expression is given in Eq. (3). The Doppler is not an explicit output of the channel model, even if it is used by the model for the phase generation. As a consequence, the echoes' Doppler has been calculated differentiating their phase measurements on two consecutive epochs. The correlation between each component of the signal and the local replica are cumulated to form a composite correlator output. The phase is assumed to vary linearly over the integration interval. The expression of the In-phase (I) and Quadra phase (Q) correlator outputs are:

$$I_P(k) = \sum_{n=1}^{N} \frac{\alpha_n(k)}{2} d(kT_s - \tau_n(k))K_{cc}(\tau_n(k) - \hat{\tau}(k))sinc\left(\pi\left(f_n(k) - \hat{f}(k)\right)T_i\right)\cos(\varphi_n(k) - \hat{\varphi}(k))$$

$$Q_P(k) = \sum_{n=1}^{N} \frac{\alpha_n(k)}{2} d(kT_s - \tau_n(k))K_{cc}(\tau_n(k) - \hat{\tau}(k))sinc\left(\pi\left(f_n(k) - \hat{f}(k)\right)T_i\right)\sin(\varphi_n(k) - \hat{\varphi}(k))$$

$$(3)$$

Where
- K_{cc} is the autocorrelation function of the spreading code.
- $\hat{\tau}(k)$ is the delay of the local spreading code
- $\hat{f}(k)$ is the frequency of the local carrier
- $\hat{\varphi}(k)$ is the phase of the local carrier

C. Validation of the LMS/Receiver coupling

The simulation platform, i.e. the combination of the LMS channel model followed by the GeneIQ receiver simulator, has been validated. In a first validation step, the LOS component of the generated received signal has been isolated from the echoes and has been processed by the simulator. This allows to check the right generation of the dynamic of the LOS signal by comparing the behavior of the tracking loops with their theoretical behavior. In this case, the received signal has been simulated for a vehicle with a constant velocity and a fixed satellite position. When the satellite to receiver distance is linearly varying, it generates a constant Doppler shift on the carrier phase and code delay, which leads to a biased estimation of the delay and phase by first orders DLL and PLL.

The code delay and carrier phase estimated by higher orders tracking loops are not biased due to a constant Doppler shift. This paper only describes the validation process of the DLL. The theoretical expression of the steady state error of a first order DLL is the following (in chips) [9]:

$$E_\infty = \frac{\Delta f_c}{4B_L} = \frac{v_0}{T_c 4 B_L c} \quad (4)$$

Where
- v_0 is the radial speed of the receiver in m/s
- B_L is the one-sided loop bandwidth of the loop filter in Hz
- $\Delta f_c = \frac{v_0}{c.T_c}$ is the code Doppler in chips/s,
- T_c is the chip duration in second

In the chosen scenario, the velocity of the vehicle is set to 20 km/h.

The satellite has an azimuth of 40° and an elevation of 50°.

The radial velocity is $v_0 = 20/3.6 * \cos(50) * \cos(45) = 2.525$ ms^{-1}.

The loop bandwidth is set to 1 Hz which is a typical value for a DLL in a GNSS receiver.

Using Eq. (4), we find a steady state error of 2.16*10^{-4} chips, which corresponds to the simulation results shown in Fig. 1.
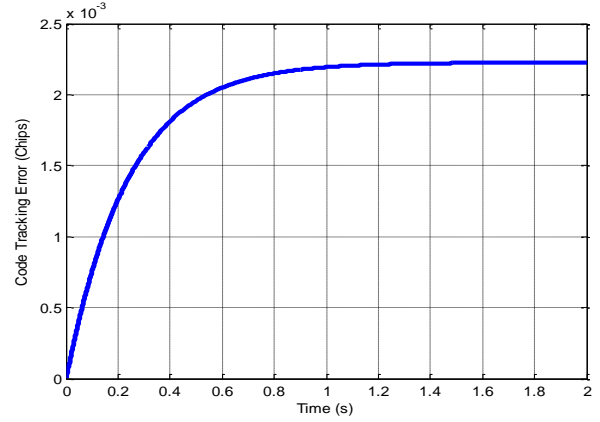

Fig. 1. Steady state error of a first order DLL for a vehicle at a constant speed on the LMS

The validation of the tracking loops can also be done by means of testing their behavior in presence of additive white Gaussian noise. In this set of simulations, the receiver simulator only is tested, and therefore the LMS channel is not connected to it. An additive white Gaussian noise is added to a simulated GPS L1 C/A signal. The simulations are conducted over 20 seconds of signal and averaged 10 times. These simulations allow to test the right consideration of the predetection bandwidth of the loops which has no impact on the steady state error due to the dynamic, and therefore was not tested. The theoretical expression of the DLL tracking error due to the thermal noise for an Early-Minus-Late Power (EMLP) discriminator which expression is given in (7), is [9], [15]:

$$\sigma_\tau^2 = \frac{B_L d}{2 \frac{C}{N_0}} \left(1 + \frac{2}{(2-d) \frac{C}{N_0} T_{int}} \right) \quad (5)$$

Where
- v_0 is the radial speed of the receiver
- T_{int} is the accumulation time
- $\frac{C}{N_0}$ is the ratio of the carrier power to the noise power spectral density in dB-Hz
- d is the chip spacing, was set to 0.5 chips

$B_{L,DLL} = 1$ Hz in the simulations.

d is set to 0.5 chips

Fig. 2 compares the theoretical expression of the standard deviation of a conventional DLL due to the additive white Gaussian noise with its simulated value. The simulated behavior of the loop is well characterized by the theoretical expression.
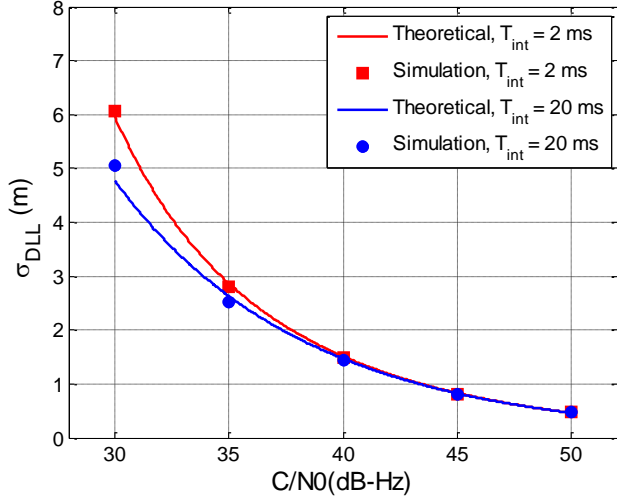
Fig. 2.   DLL tracking error due to thermal noise

Both PLL and FLL have been tested using the same approach but are not detailed in the paper.

The generation of the LOS and the right behavior of the tracking loops have been verified. The right consideration of the multipaths also has to be tested. To check that the reflections are well treated in the receiver, the LOS was set to zero and the LOS characteristics were injected in the multipath generation module. The same validations process has been conducted again on the LOS treated as an echo.

III.   PARAMETERS USED FOR THE SIMULATIONS

A. Parameters for the channel generation

The first step consists in setting the parameters for the generation of the virtual street. A typical railway in downtown Toulouse +43° 35' 58.04", +1° 27' 29.82", as illustrated in Fig. 3, was taken as a reference and reproduced in the simulator. In urban area, the railway is several meters wide because of the proximity with train station. The rows of trees and housefronts are respectively placed at a distance of 12 and 22 meters from the center of the railway.

Fig. 3.   Street model used for the channel generation

The average height of the buildings was set to 15 m and the height of the antenna was set to 4.3 m which corresponds to the standard loading gauge for trains that carry passengers (GA, GB, GB1 as defined by UIC in [10]). The typical mask angle of the buildings for this scenario is 26° for an azimuth of 90°.

According to [11], to represent the urban environment with a sufficient time resolution, the sampling frequency shall respect the relation:

$$f_s \geq \frac{8.\,v}{\lambda} \tag{6}$$

The velocity tested for the vehicle in urban area has been set to 20km/h, and therefore a 1 kHz sampling frequency that verifies the relation was chosen for the simulations. A low velocity is preferred to avoid the multipaths to be filtered by the tracking loops due to the difference between their Doppler shift and the Doppler shift of the LOS. The satellite position relative to the user is set in terms of azimuth and elevation, and will vary in order to cover most of the possible scenarios and to characterize the pseudorange error as a function of the satellite elevation.

B. GNSS signals

The characteristics of the GNSS signals that are investigated in this paper are described in this section.

1) GPS L1 C/A

The GPS L1 C/A has the following characteristics [12]:

Its carrier is located at 1575.42 MHz. The carrier is modulated by a pseudorandom code (PRN) and a navigation message by Binary Phase Shift Keying (BPSK) with a Non-return to zero (NRZ) waveform.

The spreading code is 1023 chips long and is transmitted at a rate of 1.023 Mchips/s.

The navigation message has a bit rate of 50 bit/s.

2) Galileo E1 OS

The Galileo E1 OS has the following characteristics [13]:

Its carrier is located at 1575.42 MHz.

The signal is the sum of a data channel which waveform is CBOC(6,1,1/11,+) and a pilot channel modulated with CBOC(6,1,1/11,-).

The spreading code is 4092 chips long and is transmitted at a rate of 1.023 Mchips/s.

The pilot component is modulated by a secondary code.

The data component has a bit rate of 250 bit/s.

C. Receiver model

The aim is to model the standard deviation of the code pseudorange error due to the multipaths only. In this case, no thermal noise due to the electronic component will be added to the correlator outputs. Our attention will focus on the DLL error because a basic GNSS receiver used the code measurement as the input for the navigation filter.

The normalized EMLP discriminator is preferred as it is noncoherent and therefore less affected by an abnormally large phase tracking error. It is thus more suitable to be used in urban environment.

$$D_{EMLP} = \frac{I_E^2 + Q_E^2 - I_L^2 - Q_L^2}{I_E^2 + Q_E^2} \qquad (7)$$

I_E, Q_E, I_L, Q_L are respectively the Early In-phase, Early Quadra-phase, Late In-phase, Late Quadra-phase correlator outputs of a conventional DLL.

The loop bandwidth of the DLL was set to 1 Hz which is a typical value for this loop in a GNSS receiver.

The accumulation duration for the DLL is 20 ms which correspond to the duration of one data bit for GPS L1 C/A and is typically selected when bit-synchronization has been achieved. For a fair comparison, the same accumulation duration is used for the processing of the pilot channel of Galileo E1 OS. To integrate over 20 ms, the synchronization with the secondary code is assumed.

In order to avoid the estimation of the delay to be biased due to the Doppler shift, a second order DLL is used. An FLL is preferred over a PLL for an improved robustness of the carrier tracking at the cost of a reduced precision. The bandwidth of the second order FLL is set to 5 Hz, a typical value for such a loop in actual GNSS receivers and a non-coherent arctangent discriminator is used to estimate the frequency error based on the correlator outputs. This discriminator is defined as [14]:

$$D_{ATAN} = \frac{1}{T_I} UW \left[arctan\left(\frac{Q_P(k)}{I_P(k)}\right) - arctan\left(\frac{Q_P(k-1)}{I_P(k-1)}\right) \right] \qquad (8)$$

Where

$$UW(x) = \begin{cases} x - \pi & \text{for} & x \geq \pi/2 \\ x & \text{for} & \pi/2 > x \geq -\pi/2 \\ x + \pi & \text{for} & -\pi/2 > x \end{cases} \qquad (9)$$

The accumulation duration of the FLL is set to 10 ms because the FLL requires two consecutives correlator outputs to update the frequency of the NCO. Therefore, the corrected frequency can be used for the generation of the correlator output for the DLL.

Two GPS/Galileo dual constellation receivers are considered in this paper. Both processes L1 C/A and GALILEO E1 OS but differ from each other by their front-end filters and the delays between the early and late channels, referred to as the early-late spacing, and noted *d*. The rule-of-thumb for the selection of *d* is *d*=1/BW, where BW is the one-sided bandwidth of the front-end filter in MHz.

- The first receiver is a Narrowband BPSK(1)/BOC(1,1) receiver with a front-end bandwidth of 4 MHz and a chip spacing d = 0.5

- The second receiver is a Wideband BPSK(1)/CBOC(6,1,1/11) receiver, with a front-end bandwidth of 16 MHz and a chip spacing d = 0.125. The chosen bandwidth is large enough to take into account the

contribution of the BOC(6,1) in the power spectral density of the CBOC(6,1,1/11).

The aim of this study is to determine the nominal standard deviation in a representative urban scenario due to the multipaths. The nominal scenario for the multipath error only occurs when the receiver is actually tracking the signal, and when the pseudorange errors are only due to the multipath interference phenomenon. The samples corresponding to the transient state of the loops, when the local replica is not locked on the LOS dynamic shall be excluded. Moreover the subsequent samples corresponding to a loss of lock shall also be removed not to impact the standard deviation. The receiver can self-monitor the effectiveness of its tracking thanks to detectors discussed in [9]. In this paper, as a FLL is used to track the carrier, a C/N_0 estimator is preferred over a phase lock detector:

$$\widehat{C/N_0} = A - 1 + \sqrt{A.(A-1)}$$

Where $\qquad\qquad\qquad\qquad\qquad\qquad (10)$

$$A = \frac{[mean(I_P^2 + Q_P^2)]^2}{var(I_P^2 + Q_P^2)}$$

In (10), the mean and variance are computed over 1 second. When the estimator is over a set threshold that has to be determined, it is decided that the signal is tracked and the samples shall be taken into account for the nominal standard deviation evaluation. The updating rate of the C/N_0 estimation shall be sufficiently high to quickly detect any loss of lock but shall not be too low for computation issues. 0.1 second appears to be a good trade-off between sensitivity and complexity. If the C/N_0 is over a set threshold, the latest 0.1 seconds of samples will be added to the "nominal case" vector by simple concatenation.

IV. MULTIPATH MITIGATION TECHNIQUES

Multipaths are a major challenge for the use of GNSS in urban environment, and particularly for critical and high-accuracy applications. Several reflections, that are delayed, phase shifted and attenuated compared to the LOS are processed by the receiver. These echoes distort the shape of the correlation function leading to an error on the estimation of the code delay by the DLL. The mitigation of multipath interference can be done at different level in the GNSS receiver: antenna, signal processing or position computation. The use of choke ring antennas, which filter out most of the multipath signal that are Left Hand Circular Polarized (LHCP), while allowing the direct signal which is Right Hand Circular Polarized (RHCP) to pass through, attenuates the multipath interferences. The mitigation can also be done in the GNSS receiver by modifying the design of the DLL or by adding a multipath estimation module. This paper focuses on this approach. Several techniques have been proposed in order to mitigate at the signal processing level the code pseudorange multipath error magnitude. The paper focuses on three methods: the Narrow Correlator, the Double-delta and the A Posteriori Multipath Estimation (APME). It has to be mentioned that none of these techniques mitigate the problem

of NLOS reception or improve the quality of the tracking of the carrier phase.

A. Narrow Correlator (NC)

The Narrow correlator (NC) [15], patented by NovAtel in 1991, is based on the principle of narrowing the chip spacing (d) of a conventional DLL. For a conventional DLL with an infinite bandwidth receiving an unique echo attenuated by $1/\alpha$, the maximum magnitude of the theoretical error envelope is $\alpha d/2$. Therefore the reduction of d improves the multipath resilience of the DLL. The NC also reduces the standard deviation of the DLL due to the thermal noise according to (5). The limiting factor for the choice of d is the bandwidth available for the front-end filter [16]. The estimation of the code delay is done by mean of the EMLP discriminator (D_{EMLP}).

B. Double-Delta (ΔΔ)

The Double-Delta (ΔΔ) technique uses more correlators (5 instead of 3) than a conventional early-late DLL [17]. A very early $E2(\tau)$ and a very late $L2(\tau)$ additional correlators are used, delayed by respectively $-d$ and d compared to the prompt channel.

Several different implementation of the ΔΔ technique are patented, using different discriminators, among them we can cite:

- Ashtech's Strobe Correlator [18] which uses the discriminator:

$$D = 2\big(E(\tau) - L(\tau)\big) - [E2(\tau) - L2(\tau)] \quad (11)$$

  Where $E(\tau)$ and $L(\tau)$ are the Early and Late correlator of the conventional DLL.

- Rockwell Collin's High Resolution Correlator (HRC) [17], NovAtel's Pulse Aperture Correlation (PAC) [19] which use the discriminator:

$$D = E(\tau) - L(\tau) - 0.5 * [E2(\tau) - L2(\tau)] \quad (12)$$

Both discriminators are equivalent to an early minus late discriminator, with:

$$K_{cc_{\Delta\Delta}}(\tau) = K_{cc}(\tau) - [K_{cc}(\tau + d/2) + K_{cc}(\tau - d/2)] \quad (13)$$

The correlator function $K_{cc_{\Delta\Delta}}(\tau)$ is much narrower than $K_{cc}(\tau)$, and thus, performs better in presence of multipath than a conventional DLL.

The discriminator that is used in the paper is a non-coherent ΔΔ discriminator:

$$\begin{aligned} D = {}&I_E^2(\tau) + Q_E^2(\tau) - I_L^2(\tau) - Q_L^2(\tau) \\ &-0.5 * [I_{E2}^2(\tau) + Q_{E2}^2(\tau) - I_{L2}^2(\tau) - Q_{L2}^2(\tau)] \end{aligned} \quad (14)$$

The double delta is implemented on the wideband GNSS receiver because its implementation increases the complexity of the receiver and the narrowband receiver is assumed to be a mass market low cost receiver. The NC does not increase the computation burden of the receiver and may be suitable for low cost receivers even if it requires the use of a wider front-end filter, which increases the power of the incoming signal processed.

C. A Posteriori Multipath Estimation (APME)

The A Posteriori Multipath Estimation (APME), patented by Septentrio [20], is a multipath estimation technique described in [21] and designed for GPS L1C/A. The APME does not require any modification on the design of the DLL, but relies on a multipath estimation module instead. The estimation module requires an extra very late correlator output, delayed by d with respect to the prompt channel.

The amplitude of the multipaths affecting the narrow correlator is estimated by the following formula:

$$MP = -0.42.\lambda_c\left(1 - \frac{\gamma_{+2}I_{L2}}{\gamma_0 I_P}\frac{1}{1-d}\right) \quad (15)$$

γ_{+2} and γ_0 are corrections terms that accounts for the rounding of the correlation peak due to the filtering of the secondary lobes of the incoming signal by the front-end. For a front-end with a 16 MHz bandwidth, $\gamma_0 = 1.013$.

The estimation is filtered in a low-pass filter, with a noise equivalent bandwidth of 0.1 to 1 Hz to filter out the noise [20]. The obtained correction is substracted to the code pseudorange measurements of the conventional narrow correlator DLL to reduce the multipath error.

The design of the low pass filter implemented to filter-out the noise on the estimate has a major impact on the quality of the multipath estimation. The filter output shall have a dynamic which is close to the dynamic of the multipath tracking error that results of a combination of both the multipath coherence time and the dynamic of the tracking loop. The optimal bandwidth of the low pass filter has been investigated by means of Monte-Carlo simulations on the LMS. For a vehicle driving at 20 km/h over 1 km, for several satellite positions, the low pass filter that minimizes the residual pseudorange error in the least square sense was obtained as shown in Table I. The filter implemented is a second order Butterworth filter, because it matches well with the dynamic of the second order DLL. A Bandwidth of 1.28 Hz and a linear Gain of 3.2 performs the best overall. Fig. 4 illustrates the multipath error estimation process and the reduction of the multipath interference by the APME. The APME residual error has been translated around -1 meter for a better visibility. From 20 seconds to 30 seconds the variance reduction obtained by the APME compared to a NC can be observed. Basic simulations showed that the FLL has to be replaced by a PLL when implementing the APME. A phase offset can result in a low power for the In-phase correlators compared to the noise level, which can result in an unbounded multipath estimation, derived from the quotient of two terms of noise. Nevertheless this technique could be extended to the non-coherent case by squaring the in-phase and quadra-phase correlators of the DLL. This study focuses on the implementation described in [21].

TABLE I. OPTIMAL FILTER FOR THE MULTIPATH ERROR ESTIMATION

Elevation	Azimuth		
	0•	45•	90•
50•	BW =1.28 Gain = 3.18	BW =1.24 Gain = 2.91	BW =1.28 Gain = 2.85
60•	BW =1.48 Gain = 2.79	BW =1.28 Gain = 3.15	BW =1.08 Gain = 3.29
70•	BW =1.28 Gain = 3.28	BW =1.08 Gain = 3.54	BW =1.28 Gain = 3.28
80•	BW =1.28 Gain = 3.24	BW =1.28 Gain = 3.18	BW =1.28 Gain = 3.35

higher for short and very short delays. As for the CBOC(6,1,1/11), which envelope is plotted in Fig. 7, the ΔΔ improve the multipath envelope for reflections with short to medium delays. The estimation step of the APME that is described in [21] is designed for the BPSK signal, and does not behave well for CBOC(6,1,1/11). Therefore the performances of APME are not evaluated on this signal.

The error envelope approach has a limited scope because it does not consider the multiplicity of the reflections, the distribution of the code delays which is not uniform, and the filtering by the carrier loop due to the Doppler shift of the echoes.

Fig. 5. Multipath error envelope for the narrowband BPSK(1)/BOC(1,1) receiver
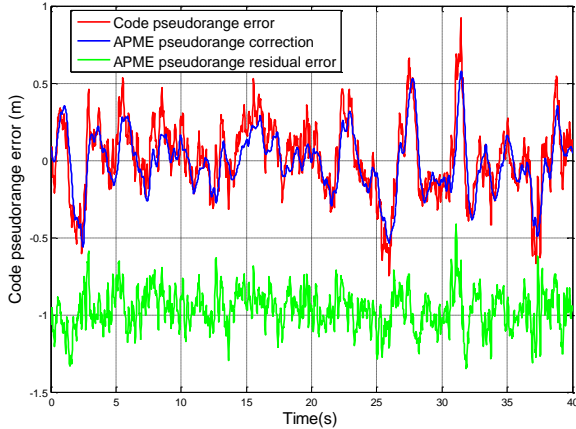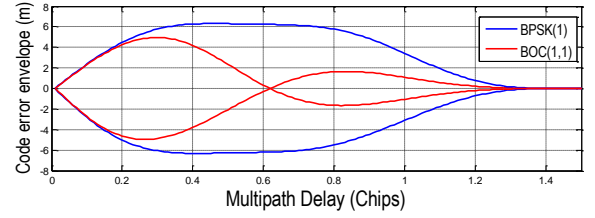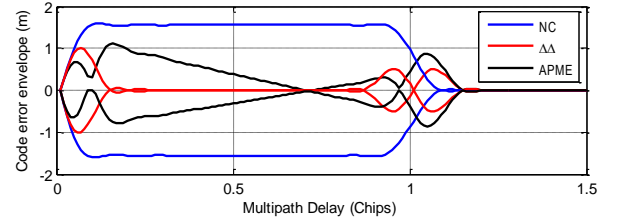

Fig. 4. Principle of the multipath mitigation by the APME. The residual error of the APME has been translated of -1 meter for a better visibility.

Fig. 6. Multipath error envelope for the wideband receiver, BPSK(1)

D. Theoretical performances

The study of the error envelope is a classical approach to evaluate the performances of the existing multipath mitigation techniques. The envelope is obtained by assuming that the signal is affected by one reflection, with a fixed attenuation, in phase or antiphase compared to the LOS. The composite discriminator is null for a delay that is neither zero, nor superior to $1+d/2$ chip, leading to an error on the code pseudorange. The multipath error envelope of the narrowband (BW = 4 MHz) receiver model, that processes BPSK(1) and BOC(1,1) with a conventional early-late DLL is plotted in Fig. 5. The Signal to Multipath Ratio (SMR) is set to 20 dB in these simulations. According to Fig. 5 BOC(1,1) outperforms BPSK(1) for long to medium multipath delays. The multipath error envelope of the dual constellation wideband (BW = 16 MHz) receiver model with multipath mitigation techniques is plotted in Fig. 6 for BPSK(1) and Fig. 7 for CBOC(6,1,1/11). The benefit of reducing the chip spacing from 0.5 to 0.125 reduces the maximum magnitude of the theoretical error by 75% for BPSK. For BPSK, the ΔΔ and APME outperforms the Narrow correlator for short, medium, and long delays multipaths. The APME does not mitigate medium to long delay multipaths, but has the envelope with the lowest magnitude for the very short delays multipaths (less than 0.1 chips). This characteristic makes this technique promising because, as stated in [21], the distribution of the reflections is
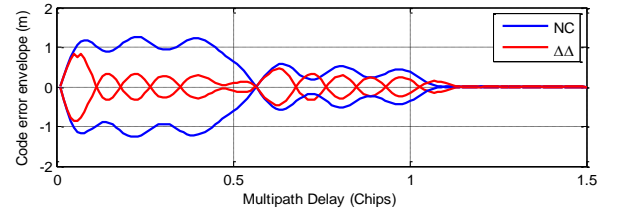

Fig. 7. Multipath error envelope for the wideband receiver, CBOC(6,1,1/11)

Among the techniques which are not investigated in this paper are the Early1/Early2 [18] tracker that processes the tracking in the area where the correlation function is less distorted, and the NovAtel's MEDLL [22] that uses several correlator to determine the amplitude, delay and phase of all the received signals, including the multipaths. The former is sensitive to the thermal noise because of the low magnitude of the correlator at the base of the correlation function and the latter increases the complexity of the receiver whereas achieving comparable level of performances as the studied techniques.

V. SIMULATION RESULTS

The simulations were conducted for a train travelling in the virtual street generated by the LMS at a velocity of 20 km/h. The satellite is positioned at eight different elevations (10, 20, 30, 40, 50, 60, 70 and 80°) and three different azimuths (0, 45

and 90°). As the topography of the street is symmetric, it is possible to limit the study at these three azimuths. The channel is generated and processed over 1km for each satellite position.

A. Threshold determination for the C/N_0 estimator

The nominal multipath error model has been calculated using the samples for which the GNSS receiver is tracking the signal. In this paper, the C/N_0 estimator given in (10) has been used as tracking detector. This estimator can easily be implemented in an actual GNSS receiver. First it is necessary to set the C/N_0 threshold at which the receiver is considered to be tracking, in presence of multipath only. Considering four thresholds (20, 25, 30 and 35 dB-Hz), the distribution of the residual error obtained after the sample selection is studied for the specific case of the narrowband BPSK(1) receiver. For a satellite which azimuth is firstly 45° and then 90°, for each elevation, and each threshold, the residual samples have been concatenated. The mean pseudorange error is plotted in Fig. 8. For elevations higher than 20°, the mean pseudorange error is sub-decimetric and does not vary with the C/N_0 threshold. For very low elevations (i.e. 20° and 10°), the distribution of the pseudorange error is not centered and its 95th percentile confidence interval is abnormally important as illustrated in Fig. 9.

The detector with a thresholds set to 30 and 35 dB-Hz effectively detect the loss of lock and exclude all the samples as illustrated in Fig. 10. The detector with a threshold set to 20 or 25 dB-Hz detects most of the biased samples, but 3% of the samples still remain not detected and are considered relevant. The magnitude of the bias is sufficiently important (several meters) to lead to a positioning failure and jeopardize the safety of the signaling system.

Fig. 10 shows the percentage of samples over the threshold, and therefore the availability of the satellite. It can be inferred from Fig. 10 that setting the threshold to 35 dB-Hz is not advisable because it reduces the availability of the satellite to less than 80 % even when the signal is tracked and that the pseudorange error is centered and has 95th percentile confidence interval lower than 2 m. The C/N_0 mask is set to 30 dB-Hz as it represents the best trade-off between the ability to detect a loss of lock and signal availability.
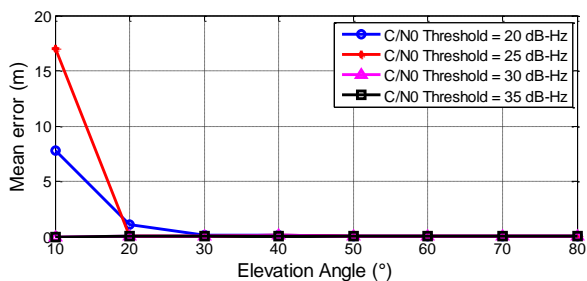

Fig. 8. Mean error of the code pseudorange error for the narrowband receiver processing BPSK(1)
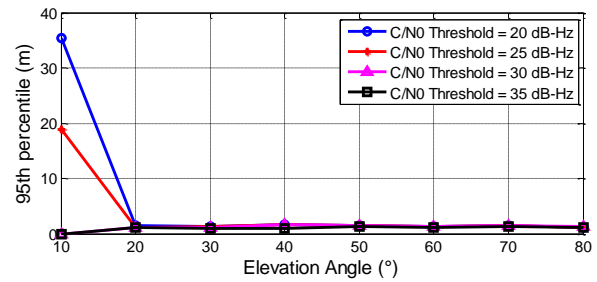

Fig. 9. 95th percentile of the code pseudorange error for the narrowband receiver processing BPSK(1)
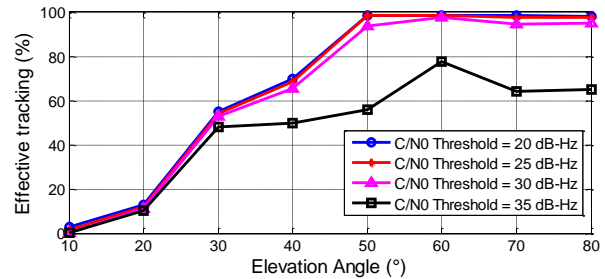

Fig. 10. Proportion of time at which the receiver is actually tracking the signal generated by the LMS simulator

The case of the 0° azimuth is not taken into account for the threshold determination as the LOS is never obstructed and the receiver is tracking for the majority of the samples. The same approach has been followed for each modulation and multipath mitigation technique but is not detailed in the paper. The same conclusion has been done for the other receivers and modulations.

In Fig. 10, it can be observed that the percentage of effective tracking for nonzero azimuths decreases with the elevation and is negligible for satellite elevation angles of 10° and 20°. To explain this phenomenon, the Signal to Multipath amplitude Ratios (SMR) histograms are plotted in Fig. 11, Fig. 12 and Fig. 13 which respectively correspond to satellite elevations of 10°, 20° and 30°. The SMR is defined as the ratio between the amplitude of the LOS and the amplitude of the strongest echo. The bimodality of the SMR distribution is characteristic of the two configurations that occur. The mode corresponding to the low SMR is the consequence of the reception of a combination of a NLOS and reflections. The mode corresponding to the high SMR is the consequence of the reception of a LOS and reflections. The NLOS reception is characterized by very low or negative SMR which lead to losses of lock of the tracking loops. It can be inferred from Fig. 11, Fig. 12 and Fig. 13 that the number of samples with very low or negative SMR increases as the elevation decreases. Therefore the amount of samples that are over the C/N_0 mask increases with the elevation.
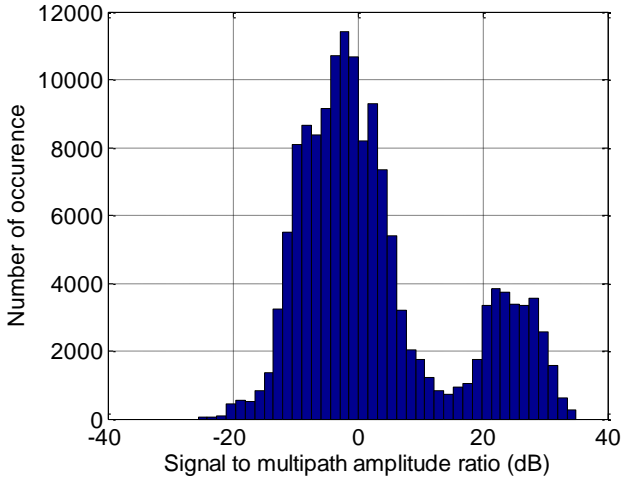
Fig. 11. Signal to multipath amplitude ratio for a satellite elevation of 10°
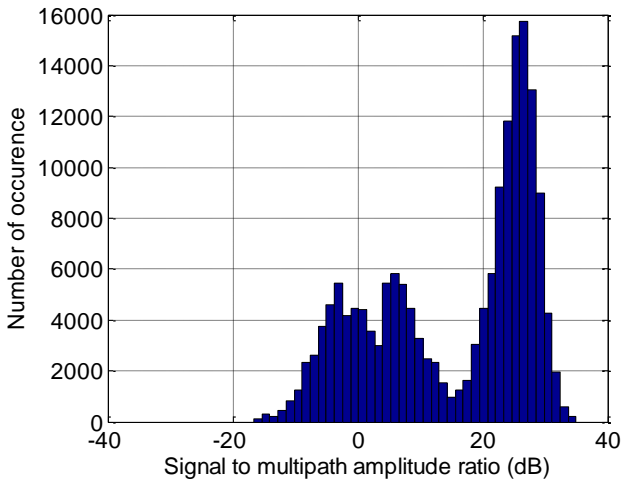

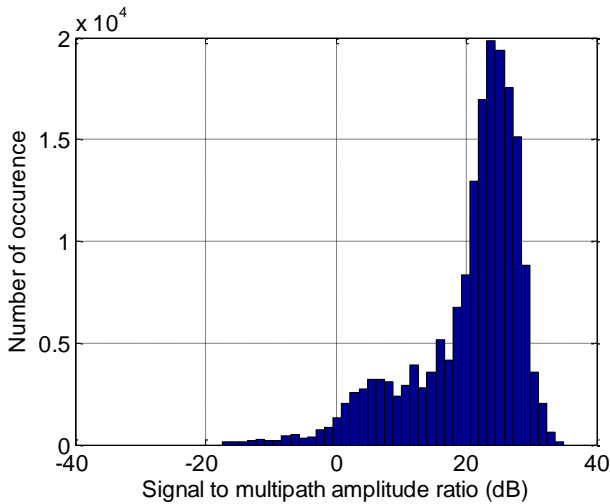Fig. 12. Signal to multipath amplitude ratio for a satellite elevation of 20°

Fig. 13. Signal to multipath amplitude ratio for a satellite elevation of 30°

B. Evaluation of the performances of the different receiver's architectures

For the simulations, the channel is generated once and each receiver's architectures and signals are processed on the same channel. The raw standard deviations of the pseudorange error are given for every azimuth. Fig. 14 illustrates the standard deviation of the code pseudorange error due to multipath. When the satellite is orthogonal to the housefronts (Azimuth = 90°) the GNSS receiver is more affected by multipath interference because this scenario is geometrically more prone for the reflections on the housefronts. According to Fig. 14, the order of magnitude of the standard deviation of the DLL error in urban is submeter. It could be inferred from that both BPSK(1) and BOC(1,1) perform the same except for the elevations that are lower than or equal to 40°. These elevations are close to or lower than the mask angle of the buildings, which means that the received signal is most of the time a NLOS embedded in statistically generated reflections. In this scenario the LOS to multipath power ratio is sufficiently low for the DLL not to be able to track the signal of interest. In the case of BPSK(1) for elevation under than 30° and azimuth different of 0°, no samples has an estimated C/N_0 over the threshold that was set to 30 dB-HZ. This phenomenon justifies the lack of points for BPSK(1) under 30° of elevation. When using the BOC(1,1) modulation, a tiny percentage of samples of the signal is tracked for low elevations.
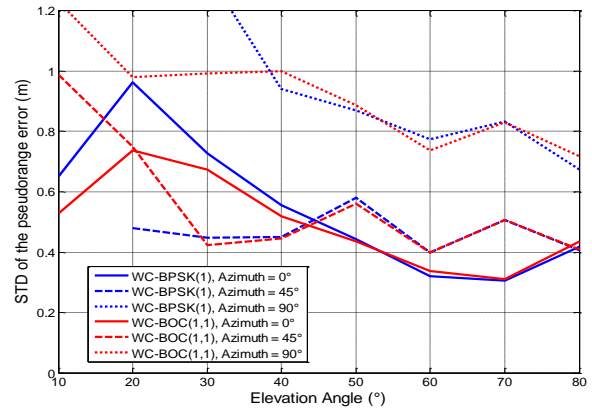

Fig. 14. Standard deviation of the code pseudorange error for the narrowband receiver

Narrowing the chips spacing of the DLL improves the robustness of the code tracking as illustrated in Fig. 15, where the channel is processed by the wideband receiver. For elevation higher than or equal to 40°, for BPSK(1), the mean reduction of the standard deviation of the multipath code error obtained by narrowing the correlators from 0.5 to 0.125 is 51.6%. This gain is more representative of the real-life performances than the theoretical gain of 75% on the multipath envelope because it takes into account the tendency of the reflection to be short delay and the multipath filtering phenomenon by the FLL due to the Doppler shift of the reflections. On the same set of data, for BPSK(1), the Double-Delta reduces the standard deviation of the code error by 29.3% on average compared to the Narrow-Correlator. The

APME performs a 37.8% reduction compared to the Narrow Correlator. When the tracking is sporadic, i.e. for low elevations, the PLL that is used for the APME instead of a FLL is not able to track efficiently which explains the lack of measurement for Azimuths lower than 30° for this technique. For every receiver's architecture and every modulation, the 95th percent confidence interval of the pseudorange error is given in annex. The APME outperforms the Double-Delta for high elevations in terms of reduction of the error magnitude as illustrated in Appendix in Table V and Table VI. At 80° of elevation, the accuracy on the pseudorange obtained by APME are 0.2898, 0.2721 and 0.4299 at respectively 0, 45 and 90° of azimuth whereas the accuracy on the pseudorange obtained by Double-Delta are 0.3859, 0.3554 and 0.6489 at respectively 0, 45 and 90° of azimuth. At low elevations Double-Delta performs better in terms of accuracy than APME.
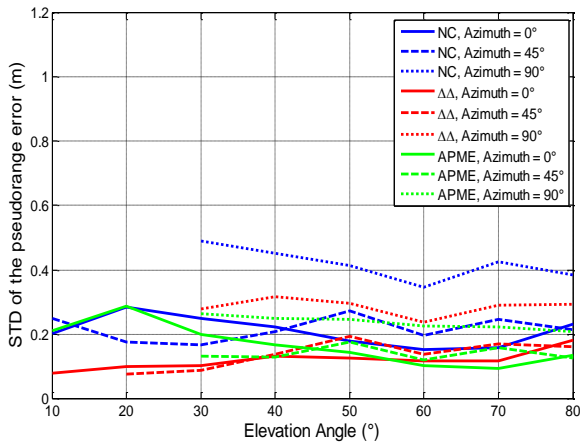

Fig. 15. Standard deviation of the code pseudorange error for the wideband receiver for the BPSK(1) modulation

Reducing the chips spacing also improves the variance of the DLL for CBOC(6,1,1/11). The double delta only improves the tracking quality for low elevations as illustrated in Fig. 16. The gain observed on the multipath envelope is not observed on the simulations on the LMS channel for high elevations.
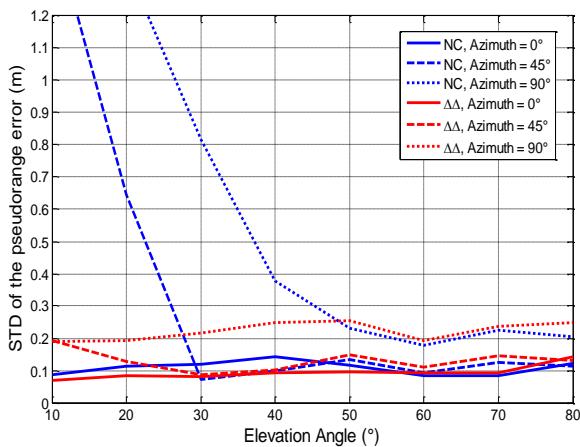

Fig. 16. Standard deviation of the code pseudorange error for the wideband receiver for the CBOC(6,1,1/11) modulation

C. Nominal multipath pseudorange standard deviations

1) Overbounding

The design of integrity monitoring algorithms requires the characterization of the actual error distribution by a known distribution. Integrity monitoring systems usually assume that the error follows a zero mean Gaussian distribution. The distribution of the raw multipath pseudorange error obtained by processing the LMS channel output is neither Gaussian nor centered. Thanks to the C/N_0 discrimination, with a threshold of 30 dB-Hz, the mean of the residual code error is sub-decimeter as shown in Fig. 8. The centered distribution still remains not Gaussian. The well-known Cumulative Distribution Function (CDF) overbounding technique described in [23] is used in this paper. The CDF overbounding technique requires the distribution to be unimodal, centered, and symmetric. The unimodality was checked by watching the histograms of the observed pseudorange error. All three assumptions are fulfilled after the C/N_0 discrimination. In real-life, the vehicle may not travel along a straight street such as what is generated in the LMS, but may face buildings when turning, or bridges, so that the satellites located in front of it can be masked. Therefore proposing a model in which the nominal multipath standard deviation is a function of the azimuth would not be relevant. For each simulated elevations, the pseudorange error from the range of possible azimuth shall be concatenated before processing the overbounding.

2) Simulation results

The results of the CDF overbounding on the pseudorange error for the narrowband receiver are given in Fig. 17. Using multipath mitigations techniques reduces the nominal standard deviation due to multipaths which can improve the protection levels and therefore improve the availability of the integrity monitoring algorithm. For elevations lower than the mask angle of the buildings, the only samples that are above the C/N_0 threshold are those obtained for a null azimuth. For this azimuth, the multipath interference is lower which results in lower sigmas as illustrated in Fig. 18. Few samples with low elevation and nonzero azimuth are effectively tracked for the wideband CBOC receiver and the overbounding process, leads to a high nominal standard deviation (as shown in Fig. 19).
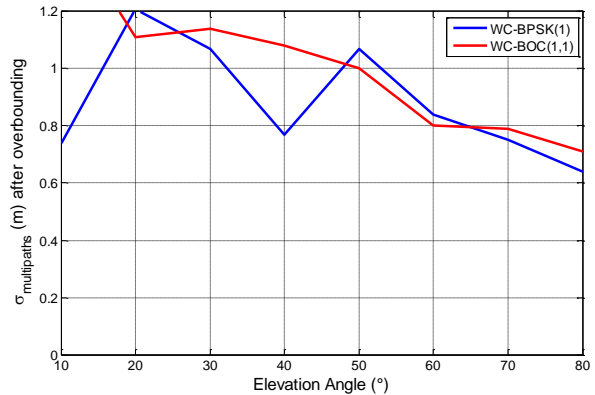

Fig. 17. Nominal multipath standard deviation for the narrowband receiver obtained after CDF overbounding
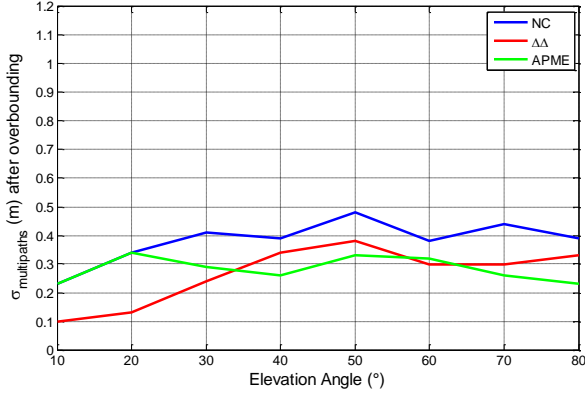
Fig. 18. Nominal multipath standard deviation for the wideband receiver obtained after CDF overbounding for the BPSK(1) modulation
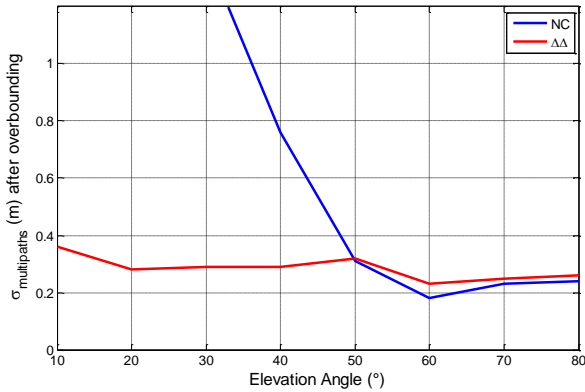

Fig. 19. Nominal multipath standard deviation for the wideband receiver obtained after CDF overbounding for the CBOC(6,1,1/11) modulation

VI. FUTURE WORK

The use of GNSS in critical applications requires an augmentation system for integrity monitoring. Ground and Satellite augmentations are not sufficient for critical terrestrial applications because they just provide alerts in case of SiS fault whereas, in urban area, the main faults are due the NLOS reception and the strong multipath interferences. Receiver Autonomous Integrity Monitoring (RAIM) techniques are able to detect and exclude faulty measurements in those situations. The classic RAIM algorithms usually assume that one pseudorange measurement is biased. In urban environment, several pseudorange may be biased simultaneously due to the receiver's environment. The use of RAIM that can detect multiple failures makes it possible to overcome the problem of simultaneous faults. The trade-off of such an approach is the augmentation of the protection levels and the calculation burden in the receiver. Another approach consists in pre excluding the faulty measurements before providing them to the integrity monitoring module. The NLOS detection may be feasible by means of Shadowmatching, [24], fisheye camera [25], or by applying masks on the C/N_0 or the elevations. The detection of large pseudorange error due to the multipath interference (LOS + echoes) is necessary. Indeed, the multipath mitigation techniques that improve the availability

of the integrity monitoring algorithms may reduce the magnitude of large multipath errors but do not necessarily prevent from potential abnormal large errors. A way to monitor the likelihood of tracking problems is the monitoring of the correlation function distortion. It can be done by means of by signal quality indicators such as the C/N_0 estimators or the metrics that are used for the detection of evil-waveforms as described by [26]. One of the proposed metrics in [26] is the simple ratio test which expression is:

$$m = \frac{I_X}{I_Y} \qquad (16)$$

Where X and Y are the fraction of chip by which the local replica is delayed compared to the prompt channel.

An analogy can be done between the differential ratio test and the multipath estimator of the APME. This estimator can be rewritten on the following form:

$$MP = 0.42 \frac{\gamma_2}{\gamma_0(1-d)} \left[\frac{I_2}{I_0} - \frac{1/\gamma_2(1-d)}{1/\gamma_0} \right] \qquad (17)$$

The APME is a particular case of Simple Ratio Test modified to be zero mean when the signal is only affected by thermal noise (by subtracting its mean), and that corrects the distortion of the correlation function due to the front-end filter thanks to the γ terms. The important ability of the APME to mitigate multipath interference can therefore be used for multipath and (potential failure) detection. Based on this assumption, further work will be focused on proposing and testing new signal quality indicators.

VII. CONCLUSIONS

A method for the estimation of the nominal pseudorange error measurement due to multipaths in urban area has been proposed. The method is based on the connection between a realistic urban channel model and a GNSS receiver simulator. This simulation platform has been validated comparing its results with its theoretical behavior in well-known scenarios. Several GNSS receiver architectures have been tested, including high end receivers that apply multipath mitigation techniques. The simulations have made it possible to compare the performances of these algorithms when processing a signal affected by reflections only. The Narrow Correlator has been demonstrated to improve the standard deviation due to multipath by 51.6% with respect to the a conventional DLL with a half chip Early-Minus late spacing. The Double-Delta and APME reduce the standard deviation due to multipath by respectively 29.3% and 37.8% with respect to the Narrow Correlator. For the different receivers and modulations, the distribution of the multipath error has been overbounded to obtain the nominal error model as a function of the satellite elevation. The simulations showed the improvement in the accuracy of the pseudorange measurement and in the nominal model when using multipath mitigation techniques for a better availability of the integrity monitoring algorithm in urban areas. The possible detection at the signal processing level of pseudorange measurement affected by non-nominal multipath interference has been discussed.

REFERENCES

[1] Safety Requirements for the Technical Interoperability of ETCS in Levels 1 & 2, UNISIG., pp 31

[2] Mocek, H ., Filip, A., Bazant, L., Galileo Safety-of-Life Service Utilization for Railway Non-Safety and Safety Critical Applications, AA(Railway Infrastructure Administration, TUDC - Laboratory of Intelligent Systems), Journal of Mechanical Systems for Transportation and Logistics, Volume 3, Issue 1, pp. 119-130, 2010

[3] K Mertens, P., Franckart, J.P., Starck, A., LOCPROL: A low cost Train Location and Signalling system for "Low Density" Lines, http://www.ertico.com/download/locoprol%20doc uments/wcrr03v3.pdf, 2003.

[4] Zheng, Y., Cross, P., Quddus, M., "The Effects of Railway Track Database Quality on the Performance of Tightly Coupled GNSS/Track Database Train Positioning System,"Proceedings of the 22nd International Technical Meeting of The Satellite Division of the Institute of Navigation (ION GNSS 2009), Savannah, GA, September 2009, pp. 2146-2155

[5] Rispoli, Francesco; Castorina, Michele; Neri, Alessandro; Filip, Ales; Di Mambro, Gino; Senesi, Fabio, "Recent progress in application of GNSS and advanced communications for railway signaling," *Radioelektronika (RADIOELEKTRONIKA), 2013 23rd International Conference* , vol., no., pp.13,22, 16-17 April 2013

[6] European Parliament, "Directive 2004/52/EC of the European Parliament and of the Council of 29 April 2004 on the interoperability of electronic road toll systems in the Community", Official Journal of the European Union, 29 April 2004

[7] Lehner, Andreas, Steingass, Alexander, "A Novel Channel Model for Land Mobile Satellite Navigation," Proceedings of the 18th International Technical Meeting of the Satellite Division of The Institute of Navigation (ION GNSS 2005), Long Beach, CA, September 2005, pp. 2132-2138.

[8] Prieto-Cerdeira, R., Perez-Fontan, F., Burzigotti, P., Bolea-Alamañac, A. and Sanchez-Lago, I. (2010), Versatile two-state land mobile satellite channel model with first application to DVB-SH analysis. Int. J. Satell. Commun. Network., 28:, no 5-6, pp. 291–315, 2010.

[9] Van Dierendonck, A. J., Global Positioning System: Theory & Applications, (Progress in Astronautics and Aeronautics), vol. 1.Washington, D.C.: AIAA, 1996, ch. 8; ISBN1-56347-106-X.

[10] UIC Leaflet 506 - Rules governing application of the enlarged GA, GB, GB1, GB2, GC and GI3 gauges"

[11] F.Perez-Fontan, M. Vazquez-Castro, C.E. Cabado, J.P. Garcia, E. Kubista, "Statistical modeling of the LMS channel," Vehicular Technology, IEEE Transactions on , vol.50, no.6, pp.1549-1567, Nov 2001

[12] IS-GPS-200-D: Navstar GPS Space Segment/Navigation User Interfaces, United States Department of Defense, Sep-2012

[13] European Commission, "European GNSS (Galileo) Open Service - Signal-in -Space, Interface Control Document Issue 1." Feb-2010.

[14] Curran, J.T.; Lachapelle, G.; Murphy, C.C., "Improving the Design of Frequency Lock Loops for GNSS Receivers," Aerospace and Electronic Systems, IEEE Transactions on , vol.48, no.1, pp.850,868, Jan. 2012

[15] Van Dierendonck, A.J., P. Fenton and T. Ford (1992), Theory and Performance of Narrow Correlator Technology in GPS Receiver, NAVIGATION: Journal of The Institute of Navigation, Vol. 39, No.3, pp. 265-283

[16] Betz, J. W. & Kolodziejski, K. R. (2000). Extended theory of early-late code tracking for a bandlimited GPS receiver, Navigation: Journal of the Institute of Navigation 47(3): 211–226

[17] McGraw, Gary A., Braasch, Michael S., "GNSS Multipath Mitigation Using Gated and High Resolution Correlator Concepts," Proceedings of the 1999 National Technical Meeting of The Institute of Navigation, San Diego, CA, January 1999, pp. 333-342

[18] Irsigler, M. & Eissfeller, B. (2003). Comparison of multipath mitigation techniques with consideration of future signal structures, P Proc. of ION GNSS, OR, USA, pp. 2584–2592

[19] Jones, J., P. Fenton, and B. Smith, (2004) "Theory and Performance of the Pulse Aperture Correlator," Proceedings of ION GPS, 2004.

[20] Jean-Marie Sleewaegen, "Method and apparatus for processing signals for ranging applications", US Patent EP 1288672 A1, 5 mars 2003

[21] Sleewaegen, Jean Marie, Boon, Frank, "Mitigating Short-Delay Multipath: a Promising New Technique," *Proceedings of the 14th International Technical Meeting of the Satellite Division of The Institute of Navigation (ION GPS 2001)*, Salt Lake City, UT, September 2001, pp. 204-213

[22] van Nee, R.D.J.; Siereveld, J.; Fenton, P.C.; Townsend, B.R.; , "The multipath estimating delay lock loop: approaching theoretical accuracy limits," Position Location and Navigation Symposium, 1994., IEEE , vol., no., pp.246-251, 11-15 Apr 1994

[23] DeCleene, Bruce, "Defining Pseudorange Integrity - Overbounding," *Proceedings of the 13th International Technical Meeting of the Satellite Division of The Institute of Navigation (ION GPS 2000)*, Salt Lake City, UT, September 2000, pp. 1916-1924.

[24] Obst, M., Bauer, S. and Wanielik, G. (2012). Urban Multipath Detection and mitigation with Dynamic 3D Maps for Reliable Land Vehicle Localization. Proceedings of IEEE/ION PLANS 2012, Monterey, CA

[25] Meguro, J., Murata, T., Takiguchi, J.-I., Amano, Y. and Hashizume, T. (2009). GPS Multipath Mitigation for Urban Area Using Omnidirectional Infrared Camera. IEEE Transactions on Intelligent Transportation Systems, Vol. 10, No. 1, 22 · 30.,

[26] Irsigler, Markus, Hein, Guenter W., "Development of a Real-Time Multipath Monitor Based on Multi-Correlator Observations, " Proceedings of the 18th International Technical Meeting of the Satellite Division of The Institute of Navigation (ION GNSS 2005), Long Beach, CA, September 2005, pp. 2626-2637

Appendix

This appendix provides the 95th percentile confidence intervals of the pseudorange error (in meters) for the various configurations of receivers and signals that are tested in the simulations.

Narrowband receiver

TABLE II.   95TH PERCENTILE CONFIDENCE INTERVAL FOR THE NARROWBAND RECEIVER PROCESSING BPSK(1)

Elevation	Azimuth		
	0°	45°	90°
10°	1.3354	-	-
20°	2.0905	1.0198	-
30°	1.5045	0.8854	2.8648
40°	1.218	0.9409	1.8602
50°	0.9151	1.1389	1.7295
60°	0.6651	0.8202	1.6515
70°	0.6074	1.0681	1.6994
80°	0.8469	0.8188	1.3734

TABLE III.   95TH PERCENTILE CONFIDENCE INTERVAL FOR THE NARROWBAND RECEIVER PROCESSING BOC(1,1)

Elevation	Azimuth		
	0°	45°	90°
10°	1.1008	1.9944	2.5634
20°	1.5908	1.568	1.9592
30°	1.4123	0.8504	2.0468
40°	1.1248	0.9425	2.0418
50°	0.9035	1.1161	1.8357
60°	0.6947	0.8278	1.5514
70°	0.6208	1.0649	1.7088
80°	0.8902	0.8226	1.4309

Wideband receiver

TABLE IV.   95TH PERCENTILE CONFIDENCE INTERVAL FOR THE WIDEBAND RECEIVER (NC) PROCESSING BPSK(1)

Elevation	Azimuth		
	0°	45°	90°
10°	0.4166	0.5763	-
20°	0.6038	0.3563	-
30°	0.5135	0.3426	1.0606
40°	0.4989	0.4309	0.9723
50°	0.3692	0.5235	0.8597
60°	0.3018	0.4023	0.7164

Elevation	Azimuth		
	0°	45°	90°
70°	0.3138	0.506	0.8578
80°	0.4739	0.4385	0.7583

TABLE V.   95TH PERCENTILE CONFIDENCE INTERVAL FOR THE WIDEBAND RECEIVER WITH ΔΔ PROCESSING BPSK(1)

Elevation	Azimuth		
	0°	45°	90°
10°	0.1669	-	-
20°	0.2314	0.1715	-
30°	0.227	0.1822	0.7064
40°	0.2864	0.3055	0.7665
50°	0.2979	0.4393	0.631
60°	0.2454	0.3158	0.5389
70°	0.2581	0.3838	0.6459
80°	0.3859	0.3554	0.6489

TABLE VI.   95TH PERCENTILE CONFIDENCE INTERVAL FOR THE WIDEBAND RECEIVER WITH APME PROCESSING BPSK(1)

Elevation	Azimuth		
	0°	45°	90°
10°	0.4423	-	-
20°	0.5887	-	-
30°	0.4158	0.2529	0.5538
40°	0.3484	0.2691	0.5439
50°	0.3039	0.3797	0.528
60°	0.2259	0.2507	0.4578
70°	0.2085	0.3506	0.4598
80°	0.2898	0.2721	0.4299

TABLE VII.   95TH PERCENTILE CONFIDENCE INTERVAL FOR THE WIDEBAND RECEIVER (NC) PROCESSING CBOC(6,1,1/11)

Elevation	Azimuth		
	0°	45°	90°
10°	0.1683	3.9713	4.4582
20°	0.2467	1.1279	3.6121
30°	0.2209	0.1529	1.6784
40°	0.3254	0.2329	0.6924
50°	0.2453	0.3004	0.5097
60°	0.1689	0.1935	0.3729
70°	0.1613	0.2589	0.4453
80°	0.2485	0.2409	0.4143

TABLE VIII. 95TH PERCENTILE CONFIDENCE INTERVAL FOR THE
WIDEBAND RECEIVER WITH ΔΔ PROCESSING CBOC(6,1,1/11)

Elevation	Azimuth		
	0°	45°	90°
10°	0.1406	0.3521	0.2685
20°	0.1803	0.2664	0.3678
30°	0.17	0.1516	0.4512
40°	0.1799	0.2166	0.497
50°	0.2077	0.307	0.5237
60°	0.1883	0.226	0.4262
70°	0.1879	0.3049	0.4952
80°	0.2989	0.2743	0.5177